

Generalization of the Iterative Perturbation Theory and Metal–Insulator Transition in Multi-Orbital Hubbard Bands

Takeo FUJIWARA, Susumu YAMAMOTO and Yasushi ISHII¹

Department of Applied Physics, University of Tokyo, Tokyo 113-8656

¹*Department of Physics, Chuo University, Tokyo 112-8551*

(Received December 6, 2002)

The iterative perturbation theory of the dynamical mean field theory is generalized to arbitrary electron occupation for multi-orbital Hubbard bands. We present numerical results for doubly degenerate E_g bands on a simple cubic lattice. The spectrum shows the electron ionization and affinity levels of different electron occupations. For sufficiently large Coulomb interaction, a gap opens in the spectrum at an integer filling of electrons and the system becomes an insulator. The present scheme is easily combined with electronic structure theory in the local spin density approximation.

KEYWORDS: strongly correlated electron systems, dynamical mean field theory, iterative perturbation theory
 DOI: 10.1143/JPSJ.72.777

The first-principles electronic-structure theory has been developed very recently for strongly correlated electron systems such as the LSDA+U method¹⁾ and the GW approximation.²⁾ The LSDA+U method can include the spin, charge and orbital fluctuation in real space whereas the GW approximation is formulated to treat the dynamical correlation of electrons. Nevertheless, these are still far from the goal since low-energy excitation of local charge fluctuation, which plays an important role near the metal–insulator transition, is not properly formulated in the frameworks of the LSDA+U method and the GW approximation. The dynamical mean field theory (DMFT) developed by Georges and Kotliar^{3–5)} has been applied to several model systems and led us to a unified picture of both low- and high-energy excitations in the anomalous metallic phase near the metal–insulator transition.

The DMFT projects a system onto the single-impurity Anderson model and this treatment is exact in the limit of the infinite dimension where the off-site Coulomb interaction can be neglected. The combination with the GW approximation is being developed to include the off-site Coulomb interaction.^{6,7)} The extension of the single impurity approximation to the cluster approximation has also been tried.⁸⁾ The effects of multi-orbitals were discussed^{9–14)} and the case of electron filling up to 1 was shown to be essentially the same as the case of the nondegenerate orbital.¹⁰⁾ The combination with the LDA or the LSDA is also desirable.^{15–19)}

To calculate the Green's functions in the DMFT, one can use several computational schemes such as the quantum Monte Carlo simulation (QMC), the iterative perturbation theory (IPT), the noncrossing approximation (NCA), the exact diagonalization (ED), the numerical renormalization group (NRG).⁵⁾ While the exact calculations such as QMC, ED and NRG may not be suitable for a wide variety of applications, the approximate ones such as IPT and NCA can be more easily combined with other calculations for real materials. The aim of this paper is to generalize the IPT for multi-orbital bands on lattices. We shall present numerical results for the doubly degenerate E_g orbitals and discuss the metal–insulator transition.

We start with the Hubbard-type Hamiltonian:

$$\begin{aligned}
 H = & \epsilon_d^0 \sum_{jm\sigma} c_{jm\sigma}^\dagger c_{jm\sigma} + \sum_{jm\sigma j'm'\sigma'} h_{mm'}^{jj'} c_{jm\sigma}^\dagger c_{j'm'\sigma'} \\
 & + \frac{1}{2} \sum_{jmm'\sigma} U_{mm'}^j n_{jm\sigma} n_{j'm'\sigma} \\
 & + \frac{1}{2} \sum_{j\sigma m \neq m'} (U_{mm'}^j - J_{mm'}^j) n_{jm\sigma} n_{j'm'\sigma}. \quad (1)
 \end{aligned}$$

In the followings, we assume that $U_{mm'}^j = U$ and $J_{mm'}^j = J = 0$, but the generalization is just straightforward. The local Green's function is defined as

$$\begin{aligned}
 G_{m\sigma:m'\sigma'}(i\omega) \\
 = \frac{1}{V} \int d\mathbf{k} [(i\omega + \mu)\mathbf{1} - \epsilon_d^0 \mathbf{1} - h(\mathbf{k}) - \Sigma(i\omega)]_{m\sigma:m'\sigma'}^{-1}, \quad (2)
 \end{aligned}$$

where $h(\mathbf{k})$, μ and $\mathbf{1}$ are the hopping matrix in \mathbf{k} -space, the chemical potential, and the unit matrix, respectively. Here we neglect the \mathbf{k} -dependence of the self-energy Σ as usual in the DMFT. For a paramagnetic and orbitally degenerate system, which is the case in the present paper, the self-energy $\Sigma_{m\sigma:m'\sigma'}(i\omega)$ and the local Green's function $G_{m\sigma:m'\sigma'}(i\omega)$ are diagonal with respect to orbitals and spins and independent of them.

The local Green's function $G(i\omega)$ is expressed as

$$G(i\omega) = [i\omega + \mu - \Delta(i\omega) - \Sigma(i\omega)]^{-1}, \quad (3)$$

with the effective hybridization function, $\Delta(i\omega)$. From the definition of “effective” medium, one defines a Green's function of the effective medium as

$$G^0(i\omega) = [i\omega + \tilde{\mu} - \Delta(i\omega)]^{-1}. \quad (4)$$

The second-order self-energy is calculated as

$$\Sigma^{(2)}(\tau) = -U^2 (N_{\text{deg}} - 1) G^0(\tau)^2 G^0(-\tau), \quad (5)$$

where N_{deg} is the degeneracy with respect to spins and orbitals (here, in case of E_g orbitals, $N_{\text{deg}} = 2 \times 2 = 4$).

The IPT was developed by Kajueter and Kotliar²⁰⁾ for a nondegenerate orbital. Here, we assume a similar form of the self-energy as

$$\Sigma(i\omega) = Un(N_{\text{deg}} - 1) + \frac{A\Sigma^{(2)}(i\omega)}{1 - B(i\omega)\Sigma^{(2)}(i\omega)}, \quad (6)$$

where $n_d = \sum_{m\sigma} n_{jm\sigma} = nN_{\text{deg}}$ and n is actually the occupation per each orbital. The coefficients A and B are

$$\lim_{i\omega \rightarrow \infty} i\omega \{ \Sigma_{m\sigma; m'\sigma}(i\omega) + \langle \{ [H_I, c_{m\sigma}], c_{m'\sigma}^\dagger \} \rangle \} = \langle \{ [H_I, c_{m\sigma}], [c_{m'\sigma}^\dagger, H_I] \} \rangle - \sum_{m''} \langle \{ [H_I, c_{m\sigma}], c_{m''\sigma}^\dagger \} \rangle \langle \{ [H_I, c_{m'\sigma}], c_{m''\sigma}^\dagger \} \rangle, \quad (7)$$

where H_I is the electron–electron interactions. The brackets $[\dots]$ and $\{\dots\}$ are the commutator and anticommutator, respectively. In the present case, the right hand side of eq. (7) is nonzero only when $m = m'$ as

$$\lim_{i\omega \rightarrow \infty} i\omega \{ \Sigma_{m\sigma; m\sigma}(i\omega) - Un(N_{\text{deg}} - 1) \} \simeq U^2(N_{\text{deg}} - 1)n(1 - n), \quad (8)$$

where we adopt a decoupling approximation $\langle n_{m\sigma} n_{m'\sigma} \rangle \simeq nn$ for $(m\sigma) \neq (m'\sigma)$. Using the second-order perturbation theory, one gets a similar result as

$$\lim_{i\omega \rightarrow \infty} i\omega \Sigma_{m\sigma; m\sigma}^{(2)}(i\omega) \simeq U^2(N_{\text{deg}} - 1)n^0(1 - n^0), \quad (9)$$

where n^0 is the occupation number for the effective medium Green's function G^0 and is determined so as to satisfy the Luttinger theorem, together with $\tilde{\mu}$. Hence the coefficient A is given by

$$A = \frac{n(1 - n)}{n^0(1 - n^0)}. \quad (10)$$

The self-energy in the atomic limit can be written down in an analytic form through the atomic Green's function for the N_{deg} -fold atomic level.²¹⁾

$$G_{mm'\sigma}^{\text{at}}(i\omega) = \frac{\delta_{mm'}}{N_{\text{deg}}} \sum_{n'_d=0}^{N_{\text{deg}}-1} \frac{(N_{\text{deg}} - n'_d)p_{n'_d} + (n'_d + 1)p_{n'_d+1}}{i\omega - \epsilon_d^0 - Un'_d + \mu}, \quad (11)$$

where $p_{n'_d}$ is the probability of finding an atom in a state of n'_d electrons present. Here the atomic levels may be given as $E = \epsilon_d^0 + Un'_d$ according to the electron occupation $n'_d = 0, 1, 2, \dots$ and all configurations are degenerate when the electron occupation is identical. If we would adopt more realistic Coulomb and exchange integral parameters $U_{mm'}^j$ and $J_{mm'}^j$ rather than the present simplified ones, the atomic levels should be split and they depend on the total angular momentum.

In order to have a precise expression for the self-energy, we assume the limit of $\beta U \rightarrow \infty$. Then the occupation probabilities of each configuration are given by

$$\begin{aligned} p_r &= 1 - (n_d - r), \\ p_{r+1} &= n_d - r, \\ p_r &= 0 : r' \neq r, r + 1, \end{aligned} \quad (12)$$

with an integer r satisfying $r < n_d < r + 1$. The self-energy in the atomic limit is then calculated as

$$\Sigma^{\text{at}}(i\omega) = Un(N_{\text{deg}} - 1) - \frac{X\{(a+b)^2 - ab - U^2\} - (a+b)ab}{(X-a)(X-b)}, \quad (13)$$

determined by requiring the self-energy $\Sigma(i\omega)$ to be correct in the high-frequency limit, $i\omega \rightarrow \infty$, and in the atomic limit, $U \rightarrow \infty$.

The self-energy in the high-frequency limit is exactly given by

where

$$\begin{aligned} X &= i\omega - \epsilon_d^0 - Ur + \mu, \quad q = n_d - r, \\ a + b &\equiv \frac{U}{N_{\text{deg}}} \{-q(N_{\text{deg}} - 1) + r\}, \\ ab &\equiv -\frac{U^2}{N_{\text{deg}}} \{N_{\text{deg}}(1 - q) - r + 2rq + q\}. \end{aligned}$$

From eq. (13) and the second-order self-energy in the atomic limit, which is calculated as

$$\Sigma_{mm'\sigma}^{(2)\text{at}} = \frac{U^2(N_{\text{deg}} - 1)n^0(1 - n^0)}{i\omega - \epsilon_d^0 + \tilde{\mu}},$$

we obtain an analytic expression for $B(i\omega)$ as

$$\begin{aligned} B(i\omega) &= \frac{i\omega - \epsilon_d^0 + \tilde{\mu}}{U^2(N_{\text{deg}} - 1)n^0(1 - n^0)} \\ &+ \frac{A(X-a)(X-b)}{X\{(a+b)^2 - ab - U^2\} - (a+b)ab}. \end{aligned} \quad (14)$$

It is easy to show that the self-energy eq. (6) with eqs. (10) and (14) is actually a simple extension of the IPT²⁰⁾ and is reduced to the known expression when $N_{\text{deg}} \rightarrow 2$. It is also similar to the results given in refs. 15 and 16 but not identical.²²⁾

To show that the present generalized IPT gives a reasonable description of the metal–insulator transition, we present numerical results for the doubly degenerate E_g bands ($N_{\text{deg}} = 4$). We consider the Slater–Koster-type tight-binding Hamiltonian of the doubly degenerate E_g orbitals on a simple cubic lattice with $\epsilon_d^0 = 0$. The effective hopping integrals are assumed only between the nearest neighbor pairs and $V_{dd\sigma} = 1/3$, $V_{dd\pi} = -2/3V_{dd\sigma}$ and $V_{dd\delta} = 1/6V_{dd\sigma}$. The relationship among $V_{dd\sigma}$, $V_{dd\pi}$ and $V_{dd\delta}$ is the scaling properties of bare two-center integrals in the LMTO method.²³⁾ Here the half band width is $D = 3(V_{dd\sigma} + V_{dd\delta}) = 7/6$. On a simple cubic lattice, there is no contribution of the $dd\pi$ interaction within the E_g orbitals due to symmetry and $V_{dd\pi}$ does not appear. Figure 1 shows the $\omega(\mathbf{k})$ -curve and the real and imaginary parts of the local Green's function for a noninteracting case ($\Sigma = 0$) with $\beta \rightarrow \infty$.

The Green's function $G(i\omega)$ is calculated in a form

$$G_{mm'}(i\omega) = \sum_{\alpha} \frac{1}{V} \int d\mathbf{k} \frac{U_{m\alpha}(\mathbf{k})U_{\alpha m'}^{-1}(\mathbf{k})}{(i\omega + \mu) - \epsilon_d^0 - E_{\alpha}(\mathbf{k}) - \Sigma(i\omega)}, \quad (15)$$

where the hopping matrix $h(\mathbf{k})$ is diagonalized to be $E_{\alpha}(\mathbf{k})$ by the unitary matrix $U(\mathbf{k})$. The \mathbf{k} -integration is carried out by using a generalized tetrahedron method. The Brillouin zone

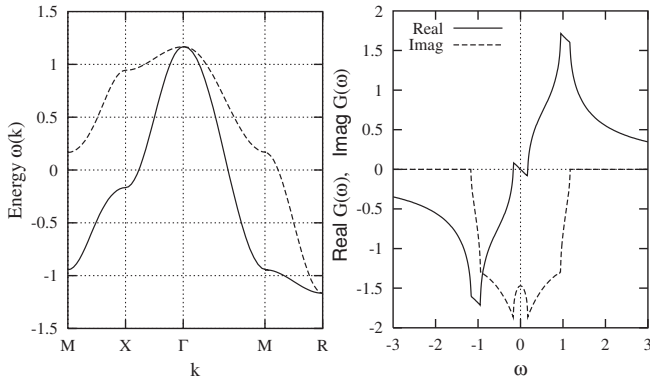


Fig. 1. The energy bands $\omega(\mathbf{k})$ along high-symmetry lines (left) and the local Green's function (right) of E_g -bands on a simple cubic lattice. The high-symmetry \mathbf{k} -points are M $(\frac{\pi}{2}, \frac{\pi}{2}, 0)$, X $(\frac{\pi}{2}, 0, 0)$, Γ $(0, 0, 0)$, R $(\frac{\pi}{2}, \frac{\pi}{2}, \frac{\pi}{2})$. The center of the band $\epsilon_d^0 = 0$ and the hopping parameters are $V_{dd\sigma} = 1/3$, $V_{dd\pi} = -2/3V_{dd\sigma}$, and $V_{dd\delta} = V_{dd\sigma}/6$. The top E_T and the bottom E_B of the bands are $E_{T/B} = \epsilon_d^0 \pm 3(V_{dd\sigma} + V_{dd\delta})$.

is divided into a set of tetrahedra and the integration is replaced by the sum of the tetrahedra and the integration within each tetrahedron of $(\mathbf{k}_1 \mathbf{k}_2 \mathbf{k}_3 \mathbf{k}_4)$. If we approximate the \mathbf{k} -dependence in the denominator and numerator by their linear interpolation, then

$$G_{mm'}(i\omega) = \sum_{\alpha, \{\mathbf{k}_i\}} \frac{6v_{\text{tet}}}{V} \int_{0 \leq u_i, u_1+u_2+u_3 \leq 1} du_1 du_2 du_3 \frac{u_1(G_1 - G_4) + u_2(G_2 - G_4) + u_3(G_3 - G_4) + G_4}{u_1(F_1 - F_4) + u_2(F_2 - F_4) + u_3(F_3 - F_4) + F_4}, \quad (16)$$

where $G_i = U_{m\alpha}(\mathbf{k}_i)U_{am}^{-1}(\mathbf{k}_i)$, $F_i = (i\omega + \mu) - \epsilon_d^0 - E_\alpha(\mathbf{k}_i) - \Sigma(i\omega)$, and v_{tet} is the volume of the tetrahedron. The integration within each tetrahedron can be written in an

explicit form. The 8×343 \mathbf{k} -points are used in the \mathbf{k} -integration within the whole Brillouin zone. The local Green's functions satisfy the relation $G_{x^2-y^2, x^2-y^2}(i\omega) = G_{3z^2-r^2, 3z^2-r^2}(i\omega)$ and $G_{x^2-y^2, 3z^2-r^2}(i\omega) = 0$ after the \mathbf{k} -integration. The Padé approximation²⁴⁾ is adopted for analytic continuation of the Green's function from the Matsubara frequency $i\omega_n$ to the real ω -axis.

The imaginary part of the local Green's function is shown in Fig. 2, for $U = 1.0, 2.2, 3.0$ and $\beta = 30$ with electron occupation $0 < n \leq 1/2$. The positive and negative energy regions, corresponding to occupied and unoccupied states, represent ionization and affinity spectra, respectively. The chemical potential decreases from $1/2U(N_{\text{deg}} - 1)$ with decreasing n from $1/2$.

In case of $n = 1/2$ ($n_d = 2$) (a half-filled case), the spectrum is very similar to that of the case of the nondegenerate band. The spectrum consists of the upper and lower Hubbard bands with the electron-hole symmetry. At the critical region (here, $U = 2.2$) one observes a sharp coherent peak at $\omega \simeq 0$. The chemical potential varies very sensitively with the occupations near $n = 1/2$ and $n = 1/4$ for $U = 1.0$ and $U = 2.2$ and it even jumps at these two occupations for $U = 3.0$. Therefore, the system becomes an insulator at $n = 1/4$ and $1/2$ when $U = 3.0$ ($U/D \simeq 2.57$). These occupations correspond to the cases of the total electron numbers $n_d = 1$ and 2 , respectively, and this is actually the case where some Hubbard subbands are completely filled and others are empty. The band gap for $U = 3.0$ at $n = 1/4$ is narrower than that at $n = 1/2$ and hence the critical U/D ratio for the metal-insulator transition may be larger at $n = 1/4$ than that at $n = 1/2$. This prediction contradicts that by QMC and, furthermore, it is presumed that the critical U/D ratio is smaller than the model of semicircular density of states in a multi-orbital case

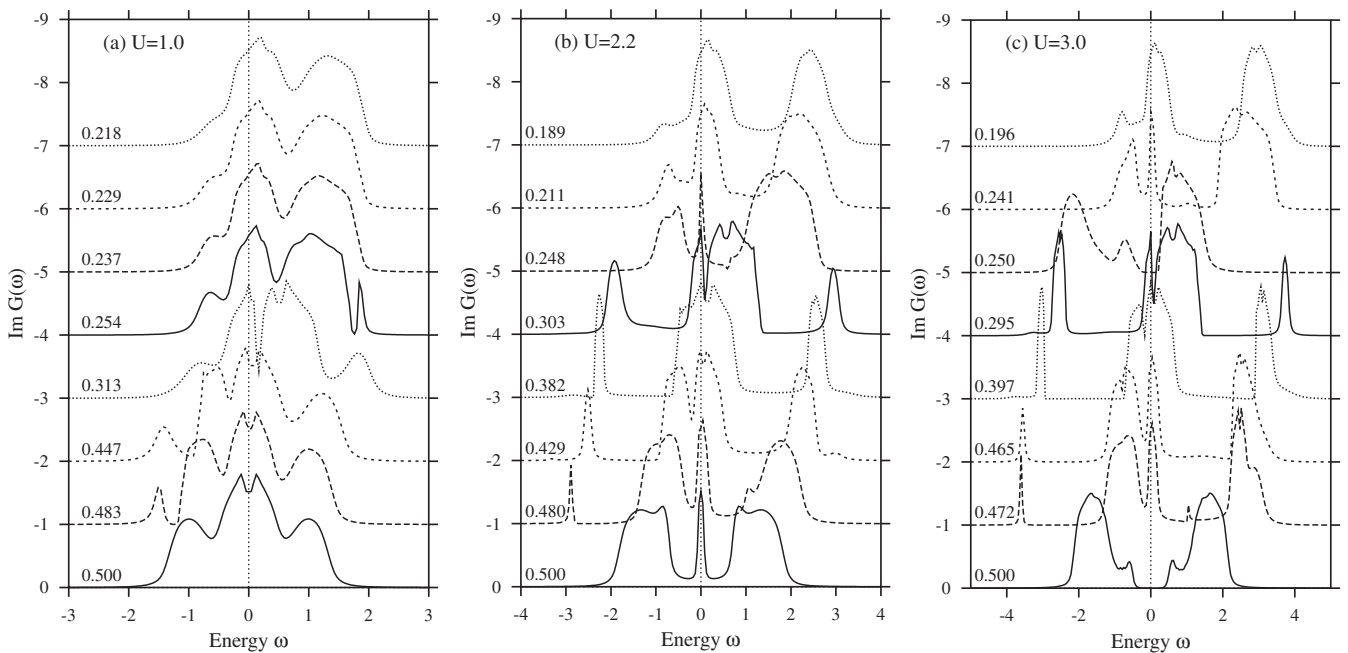


Fig. 2. The electron occupation dependence of the imaginary part of the local Green's functions for the doubly degenerate E_g band of the half band width $D = 7/6$. (a) $U = 1.0$, (b) $U = 2.2$ and (c) $U = 3.0$. The numbers in the figure denote the electron occupation n for each spectrum. The inverse temperature $\beta = 30$. The region $\omega < 0$ is occupied and that $\omega > 0$ is unoccupied. In case of the electron occupation $n = 1/4$ and $1/2$, a gap opens and the systems are in an insulating phase for $U = 3.0$.

$[(U/D)_{\text{cr}} = 3.1 \text{ at } n = 1/2]$.¹⁰⁾ This fact suggests that the critical U/D ratio would depend upon the band structure and the shape of the density of states. In an insulating case, $U = 3.0$ with $n = 1/4$ and $n = 1/2$, the self-energy shows the singular behavior $\Sigma \sim \frac{1}{i\omega_n}$ near $i\omega_n \sim 0$. On the contrary, in almost all cases, the system is metallic and the self-energy behaves as $\Sigma - Un(N_{\text{deg}} - 1) \sim i\omega_n$, which is a typical behavior of Fermi liquid. The case $U = 2.2$ is at the critical region of the metal–insulator transition, and one can see a very sharp coherent peak at $\omega = 0$ when $n = 1/4$ and $n = 1/2$. In this region, the self-energy shows the Fermi-liquid behavior.

With small hole doping, the spectrum changes very markedly, in particular for $U = 2.2$ and $U = 3.0$. A sharp peak appears at U below the lower Hubbard band, whose width depends upon the value of U and the separation from the main lower Hubbard band. In this range of $1/4 < n < 1/2$ ($1 < n_d < 2$), the lower energy state is the mixture of the ground states of $n_d = 1$ and $n_d = 2$. Then, the ionization and affinity levels for both $n_d = 1$ and 2 configurations should appear in the spectrum. The satellite structures of all configurations $n_d = 0, 1, 2, \dots$ appear but their intensity depends on the energy separation. These satellite structures originate from the self-energy, which satisfies the correct atomic limit.

When the occupation approaches $1/4$ from the above, the satellite at U above the upper Hubbard band shrinks. When the concentration n crossed the value $1/4$, i.e. $0 < n_d < 1$, the upper satellite disappears and the lower satellite merges into the main (lower) Hubbard band, since the main contribution to the spectrum comes from the mixture of $n_d = 0$ and 1, rather than $n_d = 1$ and 2 for the case of $1 < n_d < 2$. In fact, the chemical potential shifts rapidly or jumps at this concentration and the satellite grows to a main lower Hubbard band. Then the behavior for $0 < n < 1/4$ is rather similar to the case of $0 < n < 1$ for the nondegenerate orbital. The only difference is the ratio of the intensities of the lower and upper bands and it starts from the ratio of 1 : 3 near $n \sim 1/4$ rather than 1 : 1 of $n \sim 1/2$ in the nondegenerate case.

The k -dependent spectrum can be analyzed through the k -dependent Green's function $G_{mm'\sigma}(\omega, \mathbf{k}) \equiv [(\omega + \mu)\mathbf{1} - \epsilon_d^0\mathbf{1} - h(\mathbf{k}) - \Sigma(\omega)]_{mm'\sigma}^{-1}$. The band dispersion width depends sensitively upon the electron occupation. In the region of $\omega \sim 0$, the Green's function behaves as $G(\omega, \mathbf{k}) \simeq Z/\{\omega\mathbf{1} - Zh(\mathbf{k})\}$, where Z is the renormalization factor. This situation may be seen in the case of the small doping near the half filling: A small dip, which is a characteristic feature of the lattice Green's function of the E_g state, can be seen at the top of the coherent peak. The height of the coherent peak is almost equal at $n \simeq 1/2$ and $n \simeq 1/4$. Therefore the renormalization factor and the effective mass may also be equal.

It is certainly very important to have a simple scheme for solving the self-consistent Green's function in multi-orbital cases, since further generalization is needed for application to real materials showing very interesting interplay of spin, charge and orbital ordering. For that purpose, the present scheme is very practical and straightforward and, furthermore, the generalization for magnetically ordered systems and clusters containing several atoms may be quite simple.

In conclusion, we have developed a new generalization of the self-energy of the DMFT–IPT applicable to arbitrary electron occupation $0 < n < 1$ or $0 < n_d < N_{\text{deg}}$. The spectrum shows the electron ionization and affinity levels of different electron occupations. For sufficiently large Coulomb interaction, the system becomes the insulating state at an integer filling of n_d . This generalization of the IPT is easily applicable to more general cases and can be combined with the LSDA for more complex systems.

This work was supported by a Grant-in-Aid for COE Research “Phase Control in Spin-Charge-Photon Coupled Systems” and a Grant-in-Aid from the Ministry of Education, Culture, Sport, Science and Technology, Japan.

- 1) A. I. Lichtenstein, V. I. Anisimov and J. Zaanen: Phys. Rev. B **52** (1995) R5467.
- 2) F. Aryasetiawan and O. Gunnarsson: Rep. Prog. Phys. **61** (1998) 237.
- 3) A. Georges and G. Kotliar: Phys. Rev. B **45** (1992) 6479.
- 4) X. Y. Zhang, M. J. Rozenberg and G. Kotliar: Phys. Rev. Lett. **70** (1993) 1666.
- 5) A. Georges, G. Kotliar, W. Krauth and M. J. Rozenberg: Rev. Mod. Phys. **68** (1996) 13.
- 6) P. Sun and G. Kotliar: Phys. Rev. B **66** (2002) 085120.
- 7) S. Biermann, F. Aryasetiawan and A. Georges: cond-mat/0207419.
- 8) M. H. Hettler, M. Mukherjee, M. Jarrell and H. R. Krishnamurthy: Phys. Rev. B **61** (2000) 12739.
- 9) G. Kotliar and H. Kajueter: Phys. Rev. B **54** (1996) 14221.
- 10) M. J. Rozenberg: Phys. Rev. B **55** (1997) R4855.
- 11) J. E. Han, M. Jarrell and D. L. Cox: Phys. Rev. B **58** (1998) R4199.
- 12) T. Saso: J. Phys.: Condens. Matter **13** (2001) L141.
- 13) Y. Imai and N. Kawakami: J. Phys. Soc. Jpn. **70** (2001) 2365.
- 14) A. Koga, Y. Imai and N. Kawakami: Phys. Rev. B **66** (2002) 165107.
- 15) V. I. Anisimov, A. I. Poteryaev, M. A. Korotin, A. O. Anokhin and G. Kotliar: J. Phys.: Condens. Matter **9** (1997) 7359.
- 16) A. I. Lichtenstein and M. I. Katsnelson: Phys. Rev. B **57** (1998) 6884.
- 17) M. B. Zöfl, Th. Pruschke, J. Keller, A. I. Poteryaev, I. A. Nekrasov and V. I. Anisimov: Phys. Rev. B **61** (2000) 12810.
- 18) A. I. Lichtenstein, M. I. Katsnelson and G. Kotliar: Phys. Rev. Lett. **87** (2001) 067205.
- 19) K. Held, G. Keller, V. Eyert, D. Vollhardt and V. I. Anisimov: Phys. Rev. Lett. **86** (2001) 5345.
- 20) H. Kajueter and G. Kotliar: Phys. Rev. Lett. **77** (1996) 131.
- 21) J. Hubbard: Proc. R. Soc. London, Ser. A **277** (1964) 237.
- 22) Reference 15 uses the CPA results for $\Sigma^{\text{at}}(i\omega)$ and ref. 16 uses the different expression for $\lim_{\omega \rightarrow \infty} \Sigma(i\omega)$.
- 23) O. K. Andersen: Phys. Rev. B **12** (1975) 3060.
- 24) G. A. Baker, Jr.: *Essentials of Padé Approximants* (Academic Press, New York, 1975) Chap. 8.